Atmos. Chem. Phys. Discuss., 10, 109–152, 2010
www.atmos-chem-phys-discuss.net/10/109/2010/

Atmospheric Chemistry and Physics Discussions

This discussion paper is/has been under review for the journal Atmospheric Chemistry and Physics (ACP). Please refer to the corresponding final paper in ACP if available.

Quantifying pollution inflow and outflow over East Asia through coupling regional and global models

M. Lin[1], T. Holloway[1], G. R. Carmichael[2], and A. M. Fiore[3]

[1]Center for Sustainability and the Global Environment (SAGE), Nelson Institute for Environmental Studies, University of Wisconsin-Madison, Madison, Wisconsin, USA
[2]Center for Global and Regional Environmental Research, University of Iowa, Iowa City, Iowa, USA
[3]NOAA Geophysical Fluid Dynamics Laboratory, Princeton, New Jersey, USA

Received: 5 December 2009 – Accepted: 15 December 2009 – Published: 5 January 2010

Correspondence to: M. Lin (mlin26@wisc.edu)

Published by Copernicus Publications on behalf of the European Geosciences Union.

Abstract

Understanding the exchange processes between the atmospheric boundary layer and the free troposphere is crucial for estimating hemispheric transport of air pollution. Most studies of hemispheric air pollution transport have taken a large-scale perspective: using global chemical transport models and focusing on synoptic-scale export events. These global models have fairly coarse spatial and temporal resolutions, and thus have a limited ability to represent boundary layer processes and urban photochemistry. In support of United Nations Task Force on Hemispheric Transport of Air Pollution (TF HTAP; www.htap.org), this study employs two high-resolution atmospheric chemistry models (WRF-Chem and CMAQ; 36×36 km) coupled with a global model (MOZART; 1.9×1.9°) to examine the importance of fine-scale transport and chemistry processes in controlling pollution export and import over the Asian continent. We find that the vertical lifting and outflow of Asian pollution is enhanced in the regional models throughout the study period (March 2001) as contrast to the global model. Episodic outflow of CO, PAN, and O_3 to the upper troposphere during cold frontal passages is twice as great in the WRF-Chem model as compared with the MOZART model. The TRACE-P aircraft measurements indicate that the pollution plumes in MOZART are too weak and too low in the altitude, which we attribute to the global model's inability to capture rapid deep convection that develops along the leading edge of the convergence band during frontal events. In contrast to pollution export from Asia, we find little difference in the regional vs. global model transport of European (EU) pollution into surface air over East Asia (EA). Instead, the local surface characteristics – topography, land cover, O_3-VOC-NO_x chemical sensitivity – strongly influence surface O_3 responses. For instance, the O_3 response to 20% decreases in EU emissions imported into our regional model domain is strongest (0.4–0.6 ppbv) over mountainous regions and weakest (0.1–0.3 ppbv) in megacities. The spatial averaged O_3 response over EA estimated by our regional models is ~0.1 ppbv lower than global model estimates. Our results suggest that global models tend to underestimate the total budget of Asian pollutants exported

ACPD

10, 109–152, 2010

to the free troposphere given their limited ability to properly capture vertical convection and lifting. Due to the compensating effects on surface O_3 responses over downwind continents, future high-resolution hemispheric model analysis should provide additional insights into how the export and import processes interact, and will help to narrow the uncertainty of intercontinental source-receptor relationships.

1 Introduction

Pollution export and import from local to global scales is a major concern because of wide-ranging consequences for human health, ecosystems, visibility degradation, changes in radiative forcing, the hydrological cycle, and tropospheric oxidizing capacity. Findings from numerous observational and modeling studies indicate that atmospheric composition throughout the Northern Hemisphere is affected by emissions from upwind continents (e.g., Jaffe et al., 1999; Lelieveld et al., 2002; Stohl et al., 2002; Fiore et al., 2002; Akimoto, 2003). Wind speeds generally increase with height, causing pollutants at higher altitudes to be transported rapidly. Pollutants are relatively long-lived in the free troposphere due to weakened chemical loss and the absence of surface deposition. Therefore, hemispheric transport of atmospheric constituents cannot be understood without greater knowledge of exchange processes between the atmospheric boundary layer and the free troposphere. A number of key processes controlling vertical mass transport have been characterized, including the importance of midlatitude frontal passages (e.g., Cooper et al., 2002, 2004), deep convection (Lelieveld and Crutzen, 1994; Lawrence et al., 2003; Hess, 2005), and orographic forcing over complex terrains (Henne et al., 2004; Ding et al., 2009). The large-scale processes have become better understood in recent years, through integrated analysis of intensive measurement campaigns, satellite data, and ground-based observation networks with models (e.g., Jacob et al., 2003; Heald et al., 2003; Fehsenfeld et al., 2006; Singh et al., 2006, 2009). However, the importance of fine-scale mixing processes, such as by rapid deep convection, dry convection, mountain-valley breezes, land-ocean breezes,

ACPD
10, 109–152, 2010

and turbulent mixing has not been well documented, and these transport mechanisms are often not resolved in global model simulations with a typical resolution of 2°×2°.

Anthropogenic emissions over Asia have experienced a rapid increase in recent decades (Richter et al., 2005; Zhang et al., 2007). Impacts of Asian emissions on the global environment have been examined through observational and model studies focusing on key export and transpacific processes (e.g., Liu et al., 2003; Carmichael et al., 2003; Cooper et al., 2004), seasonal and episodic variability (e.g., Yienger et al., 2000; Stohl et al., 2002), and impacts over North America (e.g., Fiore et al., 2002; Zhang et al., 2008; Singh et al., 2009) and Europe (e.g., Stohl et al., 2007; Fiedler et al., 2009). Much less attention has been paid to the import of foreign emissions to Asia. A few studies using global tropospheric chemistry models estimated that European impacts on Asian surface ozone (O_3) range from 0.5–5 ppbv for various receptor areas (e.g., Wild et al., 2004; Holloway et al., 2007). In addition to these model estimates, signatures of European air masses have been detected at a remote mountain site in East Siberia (Pochanart et al., 2003). Compared to pollution export from East Asia and North America, rapid vertical exchange associated with frontal systems is weaker and less frequent over continental Europe (Stohl et al., 2002). The main transport pathway of European pollutants to East Asia occurs predominantly through the boundary layer (Wild et al., 2004), where winds are slower and chemical reactions and surface deposition may lead to additional pollutant loss. Thus, the representation of boundary layer processes and land surface characteristics is essential for estimating the import of European pollutants and subsequent impacts on surface air quality over East Asia.

It is not well understood how the key processes in tracer transport, oxidant formation and loss interact at finer temporal and spatial scales. To date, most studies of hemispheric air pollution transport have taken a large-scale perspective: using global chemical transport models (CTMs), focusing on synoptic-scale export events, and evaluating intercontinental source-receptor (S-R) relationships for relatively large regions. Under the United Nations Economic Commission for Europe (UNECE) Convention on Long Range Transboundary Air Pollution (LRTAP), the Task Force on Hemispheric

Transport of Air Pollution (TF HTAP; www.htap.org) was established to advance the understanding of hemispheric transport of air pollutants in the Northern Hemisphere. EMEP (European Monitoring and Evaluation Programme) is a scientifically based and policy driven programme under the LRTAP Convention for international co-operation to solve transboundary air pollution problems. Under the umbrella of EMEP and TF HTAP, a set of global and hemispheric CTMs was employed to quantify intercontinental S-R relationships for surface O_3 (Fiore et al., 2009; Reidmiller et al., 2009), aerosols, oxidized nitrogen deposition (Sanderson et al., 2008), mercury, and persistent organic pollutants (TF HTAP, 2007). These large-scale metrics have been used to access the impacts of intercontinental transport on human health, mortality and crops (Ellingsen et al., 2008; Casper-Anenberg et al., 2009), and will inform global air pollution policy. Thus, it is essential to understand the limitation and uncertainties in estimating intercontinental S-R relationships using large-scale models. While global CTMs provide an essential framework for estimating intercontinental scale S-R relationships, they often utilize fairly coarse spatial and temporal resolutions and simplified physical and chemical parameterizations because of computational limitations. Higher resolution regional-scale CTMs generally better simulate regional air pollution meteorology including mixing depth, wind speed, cloud and precipitation patterns, and hence improve the prediction of tracer transport and chemical evolution (e.g., Lin et al., 2008a, 2009). In addition, significant uncertainty remains regarding the representation of non-linear urban chemistry relevant to air quality in these global-scale models. Emmerson and Evans (2009) compared an explicit chemical mechanism containing ~5600 species and ~13 500 reactions with six simplified tropospheric chemistry schemes utilized in the global models. They found significant uncertainties in the chemical schemes including the treatment of N_2O_5 hydrolysis, PAN formation and sink, isoprene chemistry, and NO_3 nighttime chemistry. Therefore, it is important to evaluate the sensitivity of pollution export and import to model physics and resolution, and to determine how estimated S-R relationships vary within a region (e.g., Lin et al., 2008b; Reidmiller et al., 2009).

ACPD
10, 109–152, 2010

We employ two high-resolution regional-scale atmospheric chemistry models – the online-coupled Weather Research and Forecasting model with Chemistry (WRF-Chem v3.0) (Grell et al., 2005) and the Community Multiscale Air Quality model (CMAQ v4.6) (Byun and Schere, 2006) – to examine the export of Asian pollutants to the global atmosphere and the import of European pollution to East Asia. Both models solve for gas-phase and heterogeneous atmospheric chemical processes in a regional, three-dimensional, Eulerian framework, and they represent the two most widely used state-of-the-science models of their kind. To realistically quantify pollution import at the regional boundaries, we apply dynamic boundary conditions of relatively long-lived species derived from the global Model for Ozone and Related Tracers (MOZART v2) (Horowitz et al., 2003). We evaluate MOZART, WRF-Chem, and CMAQ with aircraft observations, examine pollution export processes and local surface O_3 responses. Intercomparison of three different regional and global models in representing pollution import and export permits a greater understanding of how global and regional processes interact, and it allows us to evaluate the role of physical parameterizations vs. resolution in contributing to model uncertainties.

We first describe the modeling framework and evaluate model simulations with aircraft measurements (Sect. 2). Our analyses seek to address two broad questions: (1) how do fine-scale vertical venting processes affect the budget of Asian pollution outflow to the global environment (Sect. 3)? (2) How sensitive is the O_3 response to mixing of imported European pollutants with local emissions and short-lived species in different receptor regions across East Asia (Sect. 4)? We then discuss the connection between these regional-to-urban scale processes and hemispheric transport of air pollution, as well as the uncertainty in intercontinental S-R relationships estimated with global models.

2 Model simulations and evaluation

2.1 Meteorological fields and emissions

The WRF regional weather forecasting model is run at 36×36 km, with eleven vertical layers in the lowest 2 km and remaining eighteen layers extending to 20 km. The online chemistry component of WRF employs the CBM-Z scheme for gas-phase chemical reactions, and the MOSAIC scheme with 4 size bins for aerosol parameterizations, and the Fast-J photolysis scheme coupled with hydrometeors, aerosols and convective parameterizations (Fast et al., 2006 and references therein). The reader is referred to Lin et al. (2009) for a detailed description of the physical options applied in the WRF meteorological predictions. Atmospheric chemical reactions and advection are calculated offline in CMAQ, driven with archived hourly meteorology fields from WRF (hereafter referred to as WRF-CMAQ). We choose the SAPRC99/AERO3 scheme for the chemistry of trace gases and aerosols in CMAQ. Regional meteorology should be considered very similar between the two regional-scale air quality models except that chemistries are dynamically solved online in WRF-Chem with meteorological predictions. The key difference between WRF-Chem and WRF-CMAQ lies in the calculation of photolysis rates, gas-phase chemistry, and aerosol dynamics.

The MOZART global model is run at ~1.9°×1.9° horizontal scale, with 28 levels in the vertical. MOZART is one of the global models participating in the HTAP emission perturbation experiments, which carried out a 20% reduction in anthropogenic emissions from East Asia (EA), Europe (EU), North America (NA), and South Asia (SA) (Fiore et al., 2009). We applied MOZART simulations with base case emissions and with 20% reductions in anthropogenic emissions of O_3 precursors from EU (scenario SR6EU). Each regional model was run twice, with temporal varying chemical boundary conditions from the MOZART base and SR6EU simulations, respectively. Boundary conditions consisted of 12 species: O_3, carbon monoxide (CO), peroxyacetyl nitrate (PAN), ethane, propane, acetone, nitrogen oxides (NO_x), sulfur dioxide (SO_2), and speciated aerosols. Ethane, propane, and acetone were selected to represent rela-

ACPD
10, 109–152, 2010

tively long-lived non-methane volatile organic compounds (NMVOCs). We evaluate the response in O_3 concentrations over EA due to changes in EU pollutants imported into our regional model domain. This approach builds on previous regional model studies by applying boundary conditions from global models to estimate the impacts of foreign emissions (Carmichael et al., 2007; Lin et al., 2008b).

The treatment of boundary layer dynamics and vertical transport processes differs between the regional and global models. MOZART is driven by meteorological fields from the NCEP reanalysis (2.5°×2.5°) taken every six hours and temporally interpolated. For WRF-Chem and WRF-CMAQ, fine-resolution meteorological fields are predicted using the WRF model driven by the NCEP Final Analyses (FNL, 1°×1°) with four-dimensional data assimilation. We choose the Yonsei University (YSU) non-local boundary layer vertical diffusion scheme for planetary boundary layer (PBL) parameterizations (Hong et al., 2006). The YSU PBL scheme includes an explicit treatment of the entrainment process of heat and momentum at the top of PBL, which resolves two major problems in other PBL schemes: too much mixing with strong wind shear, and too little mixing in the convection-dominated PBL (Hong et al., 2006). Such explicit treatment of the entrainment processes was not implemented in the boundary layer scheme of Holtslag and Boville (1993) employed in the MOZART model. Inadequate treatment of entrainment processes at the PBL top may affect the budget of pollution exchange between the boundary layer and the free troposphere. Convective parameterizations in WRF employ an improved version of the *Grell-Devenyi* ensemble cumulus scheme (Grell et al., 2002) – *Grell 3d* (cu_physics=5). The *Grell 3d* scheme allows for subsidence in neighboring columns. MOZART includes representations of shallow, midlevel and deep convection, as described in Horowitz et al. (2003) and references therein.

All models employ biomass-burning emissions from the Global Fire Emission Database (GFED v2) (van der Werf et al., 2006). Both CMAQ and WRF-Chem adopt fossil fuel emissions from Streets et al. (2003), updated for the year 2001 as described in Carmichael et al. (2007). Fossil fuel emissions in MOZART are based on EDGAR v2.0 and so representative of the early 1990s (Horowitz et al., 2003). Biomass burning

ACPD
10, 109–152, 2010

emissions in MOZART are distributed vertically up to 4 km with 70% of these emissions occurring below 2 km, other emissions for all three models are constrained in the surface model layer. Comparing the global and regional model inventories, we find that the large-scale patterns of major O_3 precursors are similar between the two inventories, with the regional inventory estimating higher emissions from urban areas and power plants (Supplementary Fig. S1: http://www.atmos-chem-phys-discuss.net/10/109/2010/acpd-10-109-2010-supplement.pdf). Total emissions of NO_x and CO in the regional emission inventory are ~15% and ~5% higher, respectively (Table 1). Total emissions of NMVOCs are close between MOZART and CMAQ, but are ~50% lower in WRF-Chem. WRF-Chem employs an online biogenic VOC emissions module based on Simpson et al. (1995) and Guenther et al. (1994), and we find that calculated isoprene concentrations over Southeast Asia in WRF-Chem are five-fold lower than CMAQ, which uses offline biogenic VOC emissions from the GEIA database (Supplementary Fig. S2: http://www.atmos-chem-phys-discuss.net/10/109/2010/acpd-10-109-2010-supplement.pdf). Discrepancies in biogenic VOC emissions, mainly isoprene, in the models may contribute to the bias of surface O_3 predictions and responses to emission reductions discussed in the remaining sections.

2.2 Overall model evaluation

Evaluating models with observations is essential for establishing credibility in their application for policy-relevant analysis. Our study focuses on March 2001 since intercontinental transport is generally strongest in the Northern Hemisphere spring season (Yienger et al., 2000; Wild et al., 2004; Stohl et al., 2002). Fiore et al. (2009) showed that the model spread in the intercontinental S-R relationships appears to be largest in spring, indicating more uncertainties than other seasons. Focusing on March 2001 also gives us an opportunity to evaluate the representation of pollutant export and chemical evolution in regional and global models against intensive measurements obtained from the TRACE-P (Transport and Chemical Evolution over the Pacific) campaign (Jacob et al., 2003). Whereas CMAQ has been well evaluated in prior studies examining chem-

istry and transport over East Asia (e.g., Uno et al., 2003; Zhang et al., 2004; Lin et al., 2008a, 2009), few studies to date have presented WRF-Chem results for this part of the world. Here, we give an overall evaluation of WRF-CMAQ, WRF-Chem, and MOZART against TRACE-P aircraft measurements, and a forthcoming manuscript (hereafter refer to as Lin et al., manuscript in preparation, 2009) will expand the intercomparison and evaluation of WRF-Chem and WRF-CMAQ over East Asia.

The models were sampled every five minutes along the flight tracks. Figure 1 shows the scatter plots of observed and modeled major tracer species (CO and ethane) and photochemical oxidants (O_3 and PAN) at altitudes below 2 km, 2–4 km and above 4 km. Both ethane and CO react relatively slowly in the gas phase and are not efficiently removed by wet processes, thus their distributions reflect mainly the source distribution and transport pathways. All models reproduce well the variations of observed ethane and CO along the flight tracks with correlation coefficients of 0.7–0.8, suggesting that large-scale transport processes were well captured in the models. Mixing ratios of CO are underestimated by a factor of two below 2 km, consistent with prior studies suggesting that CO emissions from China are higher than assumed in current inventories (Carmichael et al., 2003; Streets et al., 2006). WRF-Chem gives the greatest correlation coefficients with observations of CO and ethane among all three models, indicating the improved ability of the online-coupled climate-chemistry model to resolve the dynamic variation of regional air pollution meteorology. Section 3 will further discuss the mechanisms explaining model behavior, in particular the large differences between regional and global models in simulating vertical distributions of chemical species.

Larger differences are found in the models' simulation of the main photochemical products, O_3 and PAN (Fig. 1b), than in CO and ethane (Fig. 1a). This divergence in model estimates suggests that important questions remain regarding the complex photochemical processes involving NO_x and VOC precursors. The two regional models give higher regression coefficients than the MOZART global model, as would be expected, given the ability of CMAQ and WRF-Chem to resolve more sharply the spatial gradients in the short-lived O_3 and PAN precursors. We find that MOZART generally

underestimates the production of boundary layer O_3 and PAN in springtime, although the HTAP global model intercomparison found that most models, including MOZART, overestimate summertime O_3 (Fiore et al., 2009). Comparing the two regional models, we find that CMAQ gives better statistical scores for O_3 below 2 km, while WRF-Chem better simulates observed O_3 and PAN from 2–4 km. For near surface O_3 below 2 km, CMAQ shows correlation coefficient of R=0.89 and mean bias of MB=1.8 ppbv as compared to R=0.85 and MB=−3.2 ppbv for WRF-Chem. Our further analysis of model results with ground-based observations suggests that the current version of WRF-Chem generally underestimates ground-level O_3 over polluted regions with a relatively high NO_x/VOC emission ratio (Lin et al., 2009, manuscript in preparation), consistent with the evaluation with aircraft measurements shown here and a recent study for Mexico City (Tie et al., 2009). We recognize that the significantly lower estimates of biogenic isoprene emissions in WRF-Chem partly contribute to the negative bias in surface O_3, but the influence is restricted to Southeast Asia, the main isoprene-emitting region in springtime (Supplementary Fig. S2: http://www.atmos-chem-phys-discuss.net/10/109/2010/acpd-10-109-2010-supplement.pdf). The SAPRC99 chemical mechanism in CMAQ includes peroxyacetyl nitrate (PAN) and other higher alkyl PAN analogues, and predicts 50% higher concentrations of PAN over polluted regions than the carbon bond IV mechanism (Lin et al., 2009). Comparison with TRACE-P aircraft measurements reveals that CMAQ with SAPRC99 tends to overestimate PAN mixing ratios from 2–4 km (see Fig. 1b and Lin et al., 2009). The positive bias of PAN is particularly relevant to low-level postfrontal outflow and correlates with underestimates of O_3 in the same airstreams (figure not shown). The strong negative correlation between PAN and O_3 suggests that the CMAQ underestimate of O_3 in the postfrontal outflow is likely due to the excessive NO_x uptake by PANs. The O_3/PAN relationships at higher altitudes are generally better reproduced in the WRF-Chem model. We further examine the potential influence of the bias on the predicted O_3 responses to European emission controls in Sect. 4.1.

3 Export of Asian pollutants

3.1 Episodic nature of Asian outflow

Midlatitude cyclones tracking from west to east have been recognized as the primary mechanism for rapidly exporting air pollution from Asia and North America to downwind continents (Cooper et al., 2002, 2004; Stohl et al., 2002). Questions remain, however, as to the amount of surface emissions that make their way to the free troposphere. Here, we examine the importance of both synoptic and fine scale venting processes in controlling the total budget of Asian emissions exported to the free troposphere as represented in WRF-Chem, WRF-CMAQ and MOZART.

An important feature of the East Asian winter monsoon is frequent southeastward intrusion of cold air triggered by the Siberian anticyclone. Along with the propagation of cold fronts over China and Japan, a midlatitude synoptic wave sweeps northeastward over the East Asian coast. A total of five major frontal events are identified during the March 2001 study period following the definition of Liu et al. (2003). Figure 2 shows total zonal fluxes of CO and PAN through a wall located near 140° E, integrated from 25–40° N latitudes and from 4–8.5 km altitudes. Outflow of CO and PAN exhibits a strong episodic behavior in association with the passage of midlatitude synoptic waves. Both regional and global models capture elevated frontal outflow, with the high-resolution WRF-Chem model estimating larger zonal fluxes of CO and PAN in the middle and upper troposphere. While the global MOZART model can resolve synoptic-scale transport events, the intensity of CO fluxes in the upper troposphere is generally weaker than simulated in WRF-Chem. Vertical distribution of CO and PAN flux along 140° E shown in supplementary Fig. S3 (http://www.atmos-chem-phys-discuss.net/10/109/2010/acpd-10-109-2010-supplement.pdf) demonstrates that the pollution plumes are often excessively diluted in the global model both in the boundary layer and in the free troposphere. The enhanced lofting of Asian pollutants to higher altitude as simulated in the WRF-Chem model is recursive every 3 to 4 days throughout the study period. Total emissions of CO are only 5% higher in WRF-Chem than MOZART, which

ACPD
10, 109–152, 2010

is not enough to explain the striking discrepancies in the episodic outflow in the upper troposphere. Both anthropogenic and biomass burning emissions are distributed in the surface layer of WRF-Chem. But the injection heights of biomass burning emissions in MOZART reach up to 4 km and this explains why a few episodes (see Fig. 2) where MOZART estimates slightly higher outflow than WRF-Chem. The greatest discrepancies between the two models are found during 5–8 March when a vigorous cold front swept over East Asia and on 26 March when convective transport of Southeast Asian fire emissions dominates the CO outflow. Calculated total zonal fluxes of CO are approximately 50% higher in WRF-Chem than in MOZART for the two episodes. We focus below on the two episodes, compare model simulated vertical profiles of trace gases with observations, and examine if there are possibly missing processes in the models.

3.2 Role of rapid vertical transport

Figure 3 illustrates the WRF-Chem forecast of elevated CO in the free troposphere in association with the passage of the cold front on 7 March. A deep cyclone was located over Northern Japan (centered at 145° E, 40° N), coexisting with a Siberian anticyclone and a strong convergence band extending from Southwest China all the way to Northern Japan. We have compared the simulated precipitation pattern in the frontal zone with the multi-satellite data from the Tropical Rainfall Measuring Mission (TRMM) (figure not shown), and their close agreement suggests that the placement, geographical extent, and intensity of this frontal event are well captured by the WRF model. Mixing ratios of CO at the 5-km level reach 200–350 ppbv within the warm conveyor belt, east of the cold front. To identify the origins of the elevated CO in the middle and upper troposphere, we look at the vertical distribution of CO along ~25° N, approaching the south side of the convergence zone sweeping over West Myanmar, a heavily burned area in March 2001, and major population centers along the Yangtze River – Chongqing, Wuhang, and Shanghai (also see the thick red line in Fig. 3). Results are shown in Fig. 4 for three models, and we find that

ACPD
10, 109–152, 2010

the updraft mixing of CO is strongest in WRF-Chem and weakest in MOZART. Both WRF-Chem and WRF-CMAQ show strong CO updrafts near Chongqing extending to the upper troposphere, suggesting that some vertical lifting processes are missing in the MOZART model. Mixing ratios of CO are slightly weaker in WRF-CMAQ than WRF-Chem. This variation cannot be explained by the difference in biogenic isoprene emissions (Supplementary Fig. S2: http://www.atmos-chem-phys-discuss.net/10/109/2010/acpd-10-109-2010-supplement.pdf) because oxidation of isoprene in CMAQ will lead to larger CO outflow. We suspect that the temporal resolution of convective processes, solved every three minutes in WRF-Chem, will play a role. The WRF-Chem panel in Fig. 4 also shows the vertical distributions of equivalent potential temperature (θ_e), calculated using the formula from Bolton (1980). Equivalent potential temperature provides a measure of the instability of the column of air because it always increases with increasing temperature and moisture content. In stable conditions, θ_e increases with altitude. If θ_e decreases with height, convection can occur, as is the case, above Myanmar (90–100° E) and Chongqing (105–110° E), indicating convective conditions. In particular, deep convection developed near Chongqing, leading to strong upward transport of CO to the upper troposphere. The strong lofting of CO occurred within just a few hours and was rapidly pushed offshore by the strong westerly winds.

This event was sampled by the NASA DC-8 platform flying through the frontal region near the East China coast on 7 March. Figure 5 compares the observed and modeled vertical distributions of CO, O_3 and PAN along the flight path. It can be seen that the observed CO distributions along the flight path clearly show outflow within the frontal zone (4:00~6:00 UTC) extending to altitudes of ~6–8 km. Impacts of the primary airstreams that composed this cyclone, e.g. strong advection and lifting in the warm conveyor belt (03:00–06:00 UTC) and dry intrusion of upper level background air (08:00–10:00 UTC), are remarkably well simulated in the high-resolution WRF-Chem model. WRF-Chem predicted outflow of CO to the western Pacific exhibits a complex structure appearing in three vertical layers: mixing of fresh emitted emissions capped in the boundary layer below 1 km; background outflow of CO originated from the coastal region of China con-

fined below ~3 km over the prefrontal region; and large-scale outflow above 4 km within the frontal zone. While the global MOZART model generally captures the large-scale lifting of CO during 04:00–06:00 UTC, the plume is diluted and appears in the wrong place, strongest in the lower free troposphere rather than in the middle and upper free troposphere as in WRF-Chem and in the observations.

Sources of CO in the layers above 4 km sampled by the aircraft are mainly attributable to biomass burning emissions in Southeast Asia (Carmichael et al., 2003) and to industrial emissions along the convergence band as illustrated in Fig. 3. All models in this study applied the same dataset for biomass burning emissions (see also Sect. 2 and supplementary Fig. S1: http://www.atmos-chem-phys-discuss.net/10/109/2010/acpd-10-109-2010-supplement.pdf). The striking bias in simulating vertical distributions of trace gases illustrated here is primarily due to the representation of key meteorological processes in different models. Deep convection is an important mechanism for vertically transporting Southeast Asia biomass burning emissions out of the atmospheric boundary layer into the middle and upper troposphere (Duncan et al., 2003; Hess, 2005). The occurrence of cold fronts tends to enhance subtropical and tropical deep convection because of the intense low-level convergence along their leading edge (Garreaud, 2001), as is the case simulated in the WRF model. We find consistent enhancement of deep convection embedded in rising airstreams for multiple warm conveyor belt transport events in March 2001 (Supplementary Fig. S3: http://www.atmos-chem-phys-discuss.net/10/109/2010/acpd-10-109-2010-supplement.pdf). MOZART diluted and misplaced the plumes at the lower free troposphere during these events, suggesting its inability to resolve this rapid deep convection that develops along the leading edge of the convergence band. In addition, we find that the export of biomass burning emissions from Southeast Asia during the 26-March episode is likely enhanced by orographic forcing over the complex terrains in Myanmar and Southwest China (figure not shown).

The export of CO emissions during the frontal event discussed above is associated with elevated mixing ratios of major photochemical oxidants O_3 and PAN (Fig. 4). Mix-

ing ratios of O_3 in the intense CO plume exceed 60 ppbv, comparable to background outflow confined below 4 km in the prefrontal region. While these features are captured in the WRF-Chem model, MOZART significantly underestimates mixing ratios of O_3 and PAN within the frontal region, as expected given the weak vertical mixing in the global model. PAN is of great importance to the impacts of long-range transport because PAN acts as an effective reservoir for NO_x and its thermal decomposition can lead to O_3 production over remote areas far away from emissions source regions (Moxim et al., 1996). Recent aircraft studies have detected strong O_3 enhancement driven by PAN decomposition in subsiding plumes containing large amount of PAN formed over upwind continents (e.g., Heald et al., 2003; Real et al., 2007; Zhang et al., 2008). Therefore, MOZART's underestimate of PAN both in the surface level (Fig. 1b) and in elevated transpacific plumes (Fig. 5) will lead to a weaker impact of Asian pollution on background O_3 over downwind continents. Supporting this conclusion, the NA and EU O_3 response to a 20% decrease in EA emissions is ~0.1 ppbv lower in MOZART than the 15-model ensemble mean for March (Fiore et al., 2009).

The inability of MOZART to accurately simulate pollutant venting through deep convection and orographic forcing over the continent causes the model to misplace an Asian outflow plume along 140° E in the upper troposphere (Fig. 6). Throughout the study period, we find that the plumes in MOZART are generally more diluted both in the boundary layer and the upper troposphere. During the intense frontal events on 7 and 26 March, the zonal flux of CO differs by a factor of two in the upper troposphere between the two models. WRF-Chem yields strong and intensified CO fluxes extending to the upper troposphere, where the stronger winds can rapidly transport these airmasses across intercontinental distances. The CO/O_3 ratios in the pollution plumes are also shown in Fig. 6. Both plumes on 7 and 26 March show strong CO outflow in the middle and upper troposphere, but the O_3 enhancement is different resulting from airstreams drawing from regions with different surface emissions. The lower CO/O_3 ratios for the 7-March plume, which originated from Southwest and Eastern China, indicate elevated O_3 mixing ratios in the troposphere. The 26-March plume originated from biomass

burning regions in Southeast Asia, however, did not show this O_3 enhancement, consistent with analysis of boreal fire plumes in Alaska and Canada (Singh et al., 2006). Hudman et al. (2007) attributed the weak O_3 enhancement in biomass burning plumes to rapid conversion of the emitted NO_x to PAN.

3.3 Discussion on export uncertainty

A number of previous studies suggested that vertical transport and distribution of O_3 and its precursors respond to convection differently in different models (e.g., Doherty et al., 2005; Lawrence et al., 2003; Kiley et al., 2003; Zhao et al., 2009). Convective systems encompass small-scale fair weather cumuli, active thunderstorms, and mesoscale convective systems (Cotton et al., 1995). The corresponding lifetime of these systems increases with their size from minutes to about half a day. Therefore, the representation of convective transport and associated clouds and precipitation processes is typically sensitive to both the model's spatial and temporal resolution. The high-resolution meteorological prediction with WRF in combination with four-dimensional data assimilation technique, as opposed to the coarse NCEP reanalysis for MOZART, is one of the key reasons for the improved simulation of tracer vertical transport in WRF-Chem and WRF-CMAQ. In addition, the WRF simulations in this study employed the new Grell 3d scheme for convective parameterization (Grell et al., 2002), and evaluation of chemical compositions presented here illustrates the capability of this new convective scheme to closely simulate vertical exchanges of air masses. The convection scheme applied in MOZART need to be further evaluated and improved in future research. We conclude that the differences arising from driving meteorology resolution, convective parameterizations, and orographic effects are responsible for the contrasting effects of updraft transport displayed by the regional and global models.

Based on available data, we are only able to evaluate model skill at capturing episodic outflow, but we would expect that the limitations in the ability of global models to resolve surface-to-free troposphere exchange and chemical processing would underestimate outflow on a consistent basis. Results presented by Liu et al. (2003) show

that the global GEOS-Chem model, which has been widely used to quantify intercontinental transport of air pollution (e.g., Fiore et al., 2002; Heald et al., 2003; Li et al., 2003; Zhang et al., 2008), also misplaced the 5–8 March pollution plume in the lower free troposphere. Recent model analysis of observations from the Intercontinental Chemical Transport Experiment – Phase B (INTEX-B) campaign, conducted in spring 2006 over the Northeast Pacific, found that most current global-scale models have limited ability to reproduce discrete Asian gas and aerosol plumes arriving at the North American west coast (Singh et al., 2009; Dunlea et al., 2009). We suspect that this is partly due to inadequate treatment of small-scale venting over the Asian continent. These smaller-scale venting mechanisms have greatest importance in warm seasons when large-scale stirring by synoptic systems is diminished. Kiley and Fuelberg (2006), using a fine resolution regional meteorological model (MM5), shows that weak, midlatitude cyclones in summer are capable of producing vertical forcing as great or greater than much stronger cyclones over North American east coast. Analysis of aircraft field campaigns over North America demonstrated that the models are able to capture typical correlations between tracers and main features of anthropogenic outflow from North America (e.g., Li et al., 2004; Parrish et al., 2004; Fang et al., 2009). However, results presented in Fang et al. (2009) (Fig. 8) show that an elevated CO plume in excess of 500 ppbv extend to 6–10 km and the MOZART global model underestimated CO by a factor of five. They attributed this significant bias to excessive dilution of the fire plume or inadequate treatment of pyroconvection that injected strong boreal fire emissions into the upper troposphere and lower stratosphere (Turquety et al., 2007). Other studies have suggested that plumes are often diluted more quickly than observed due to numerical diffusion and poor resolution in the global-scale tropospheric chemistry models (Heald et al., 2003; Pfister et al., 2006). In terms of European outflow, Henne et al. (2004, 2005) revealed a strong influence of topographic venting on O_3 mixing ratios in the lower free troposphere over and downwind of the Alps, and suggested that orographic forcing is expected to play an important role in O_3 production and outflow on a European scale.

ACPD
10, 109–152, 2010

Enhanced lifting of surface pollutants to the free troposphere where it can undergo rapid long-range transport – as observed in aircraft studies and simulated in the regional models – might not immediately contribute to the degradation of surface air quality over downwind continents. However, pollutants are generally long-lived in higher altitudes and the mixing into the background troposphere air can eventually lead to increasing levels of background atmospheric constituents over downwind continents (Fiore et al., 2002). The dilution of intense plumes in large-scale models makes it especially difficult to quantify the impacts of episodic transport (Wild et al., 2004; Fang et al., 2009). Yienger et al. (2000), using a global atmospheric chemistry model, estimate that major Asian pollution events are very common in the middle and upper troposphere above the United States, but perhaps only 3–5 of these events directly impact the atmospheric boundary layer along the US. West Coast during a typical February–May period. However, our understanding of intercontinental transport impacts on surface air quality would greatly benefit from further studies of small-scale mixing into the boundary layer using high-resolution models and intensive three-dimensional field measurements. The California Air Resources Board (CARB), the National Oceanic and Atmospheric Administration (NOAA) and the California Energy Commission (CEC) are proposing a joint field study of atmospheric processes over California and the Eastern Pacific Coastal Region in 2010 (NOAA, 2008). Three-dimensional sampling of ozone and aerosols from lidar, aircraft and research vessel from this study will provide a unique opportunity to examine the entrainment of free tropospheric air into the atmospheric boundary layer affected by orographic flow in California's central valley.

4 European impacts over East Asia

We first discuss the spatial sensitivity of monthly mean surface O_3 responses over EA to changes in EU pollutants imported into our regional model domain (Sect. 4.1). Time evolution of EU sources over China and Japan is further examined at two representative sites (Sect. 4.2). Discussion of surface O_3 responses in this sec-

tion will focus on model results from CMAQ and MOZART for two reasons. First, total emissions of NMVOCs are similar between CMAQ and MOZART, and CMAQ has been found to perform better than WRF-Chem in capturing surface O_3 production (see Sect. 2). Second, CMAQ applies hourly-varying chemical boundary conditions, consistent with the output frequency of chemical concentrations in MOZART, while WRF-Chem employs the boundary conditions at six-hour interval. Supplementary Figs. S4, S5 (http://www.atmos-chem-phys-discuss.net/10/109/2010/acpd-10-109-2010-supplement.pdf) present WRF-Chem results analogous to the CMAQ and MOZART findings discussed in the text.

4.1 Spatial sensitivity of ozone responses

Figure 7 shows MOZART and CMAQ calculated EU enhancements on surface O_3 over EA averaged over 1–15 March. The large-scale spatial pattern of EU impacts over EA is similar between MOZART and CMAQ. However, the O_3 response to changes in EU pollutants imported into our regional model domain exhibits a large local and regional variability, indicating the important role of surface processes, which differ from region to region. For example, the CMAQ regional model clearly demonstrates the sharp gradients of enhanced O_3 loss through surface deposition over the land as opposed to over the ocean, due to uptake by plants and stronger turbulence. While MOZART generally captures the broad land vs. ocean difference, its limited ability to resolve coastal lines leads to overestimate of EU enhancements on surface O_3 over the coastal regions of Eastern China, South Korea, and South Japan. Surface topography can enhance ventilation of surface emissions through mountain-valley wind systems as well as suppress horizontal transport across mountain ridges. CMAQ shows that EU enhancements on surface O_3 are 0.5–1.0 ppbv stronger in northwest mountainous regions than in the North China Plains (30–45° N, 115–125° E), although both regions are located along major springtime transport pathways of European pollutants. Consistent with the results presented here, Jaffe et al. (2003) showed that the impacts of Asian dust are stronger in surface air over the Rocky Mountains of the western United States. Moun-

tain top entrainment of free tropospheric air and weakened surface depositional and chemical loss affected by the sharp orographic gradients are better resolved in fine resolution models; they are key factors contributing to enhanced O_3 responses over these regions.

Subsequent mixing of imported pollutants with local emissions and short-lived radicals affects the relative contribution of foreign sources to local surface air quality as well. For instance, the CMAQ regional model detected that EU O_3 enhancement is lowest over surface air in megacities such as Beijing, Seoul and Tokyo. In these areas, European O_3 imported into the regional model domain is titrated by high local emissions of NO_x. Foreign enhancement on local O_3 budget can occur through both direct transport and production driven by PAN decomposition. Local/regional VOC reactivity, VOC/NO_x ratios and sources of short-lived radicals play important roles on the O_3 production efficiency driven by foreign PAN decomposition. Total emissions of NO_x are 15% lower in MOZART, which leads to a relatively higher VOC/NO_x ratio in the global model. Thus, O_3 production tends to be in the NO_x-limited regime in MOZART. Under such conditions, the O_3 production efficiency driven by European PAN decomposition is likely low in MOZART. In contrast regional models simulate O_3 formation over Northeast Asia to be in the NO_x-saturated regime (Carmichael et al., 2003). Increasing NO_x from European sources has a relatively weaker influence on local O_3 production because of increased termination from OH+NO_2 rather than OH propagation occurring by OH+VOC (Seinfeld and Pandis, 2006). Additional analysis by changing PAN boundary conditions only will provide further insights into the role of PAN formed in upwind continents in changing local O_3. A 20% decrease in European pollutants imported into the CMAQ regional domain induces a 0.3 ppbv response in spatially averaged surface O_3 over EA. Fiore et al. (2009) shows that the intermodel difference in the EA O_3 response to 20% EU emission changes is largest in March, ranging from 0.1–0.7 ppbv. The CMAQ estimate falls within the range of global model estimates, but appear to be 0.1 ppbv lower than MOZART and the 15-model ensemble mean (0.4 ppbv).

ACPD
10, 109–152, 2010

The estimate of O_3 S-R relationships by perturbing regional emissions is sensitive to model representation of the nonlinear photochemical cycle, as chemical mechanisms have been found to substantially impact model predictions of photochemical oxidants and the sensitivity of O_3 responses to controls in NO_x and VOC emissions (e.g., Lin et al., 2009; Emmerson and Evans, 2009). Our estimates of the sensitivity of O_3 responses to imported foreign oxidants strongly depend on the chemical scheme employed in the model and the sources of HO_x and NO_x in the local/regional environment. For example, the CMAQ model employing the SAPRC99 mechanism estimated approximately 0.5 ppbv higher O_3 responses over the main transport pathways of European pollutants than WRF-Chem with the carbon-bond mechanism of Zaveri et al. (1999) (CBM-Z) (Supplementary Figs. S4 and S5: http://www.atmos-chem-phys-discuss.net/10/109/2010/acpd-10-109-2010-supplement.pdf). We have also conducted sensitivity experiments using the RACM chemistry in WRF-Chem, and the O_3 response over land is consistent with the response using CBM-Z although the response over the ocean is ~1.0 ppbv higher. We recognize that the discrepancies in biogenic VOC emissions between CMAQ and WRF-Chem affect the magnitude of the Asian surface O_3 responses to European emission controls, but this influence is limited to Southeast Asia where biogenic emissions in March are highest in our study domain (Supplementary Fig. S2: http://www.atmos-chem-phys-discuss.net/10/109/2010/acpd-10-109-2010-supplement.pdf). Instead, the differences in the O_3-NO_x-VOC chemistry, VOC oxidation rates and radical cycling in the chemical mechanisms play a major role in controlling the sensitivity of O_3 responses in Eastern China. The SAPRC99 mechanism in CMAQ considers a larger set of VOC species than the carbon-bond mechanisms and SAPRC99 is generally considered to be a more reactive mechanism than others. We conclude that the strength of surface O_3 responses to reductions in foreign emissions is very sensitive to atmospheric constituents in the local/regional environment and to the representation of this environment in the models.

4.2 Time evolution of European impacts over China and Japan

Venting through the top of the atmospheric boundary layer often involves small-scale entrainment processes not directly simulated on the global scale. The representation of boundary layer processes and associated diurnal boundary layer depths is essential for evaluating hemispheric transport impacts on surface air quality. To examine the free troposphere-to-surface exchange processes importing European emissions to surface air, we look at the temporal evolution of the vertical profiles of European CO and O_3 at two regionally representative sites: Mount Hua (34.5° N, 110.1° E, 2064 m) in Central China and Mount Happo (36.7° N, 137.8° E, 1850 m) in Central Japan. Regular measurements of ground-level O_3 have been set up in Mount Hua since 2004 to monitor regional air pollution in China (Li et al., 2007; He et al., 2008). Mechanisms controlling surface O_3 at Mount Happo have been widely examined in prior studies, including O_3 formation, seasonality and diurnal variations (e.g., Lin et al., 2009), impacts of intercontinental transport (Wild et al., 2004), and long-term changes (Tanimoto et al., 2009). Here, we focus on the importance of boundary layer mixing and fine-scale oxidant formation processes in affecting the O_3 and CO responses at these two sites to reductions in European emissions.

Figure 8 illustrates that CMAQ, by employing chemical boundary conditions from MOZART, simulates major events of European influence over China and Japan in association with the passage of cold fronts as discussed in Sect. 3. Mixing depths between the two models are very similar, and we do not see a clear relationship between surface pollution enhancements and mixing depths. MOZART and CMAQ calculated European sources of CO at Mount Hua and Happo are very similar in large-scale pattern, and both show the plume arriving at the same time. CMAQ shows ~10 ppbv lower European CO at both sites. European impacts at Mount Hua are primarily episodic, affected by the intrusion of cold air triggered by the Siberian anticyclone. Passage of the vigorous cold front during 5–8 March (Fig. 3) results in 40–50 ppbv enhancements in CO at Mount Hua by European emissions. The timing of maximum European influence

ACPD
10, 109–152, 2010

at Mount Happo appears two days later, corresponding to the arrival of cold frontal air masses. In addition to episodic transport, European emissions also contribute approximately 20–30 ppbv to background CO at Mount Happo. This is because Japan is on the major springtime pathway of southeastward flow after trans-Eurasia transport across 120° E (Wild et al., 2004).

The difference in O_3 responses is larger than the difference in CO between the models (Fig. 9). Descending Siberian air during 5–8 March leads to 3–5 ppbv European enhancements in surface O_3 at Mount Hua. This is shown both in CMAQ and MOZART, although CMAQ gives much lower O_3 responses to European emissions in both surface air and higher altitudes, in response to the relative sources of short-lived radicals (as discussed in Sect. 4.1). A large difference is found in O_3 responses in the middle troposphere as well. Overall, both regional models suggest lower impacts of European sources, as compared to global model estimates, on tropospheric O_3 over Japan. European O_3 and its precursors imported into regional models are subjected to faster chemical loss and destruction.

5 Conclusions

This study employs two state-of-the-science regional atmospheric chemistry models (WRF-Chem and CMAQ) coupled with a global chemical transport model (MOZART) to examine how chemical transport, oxidant formation and loss interact at finer temporal and spatial scales, and the sensitivity to model physics. The importance of synoptic to urban scale processes on the rapid export of Asian pollutants and the import of European pollutants over East Asia are evaluated using meteorology for March 2001. While our work was motivated by an interest in the role of regional-scale atmospheric processes and model resolution, it is critical to consider these findings in light of model uncertainties and structure (online vs. offline). Regional and global model simulations of chemical species are carefully evaluated with intensive aircraft measurements from the TRACE-P field campaign. We found that WRF-Chem, an online climate-chemistry

model, gives the highest correlation coefficients among all three models, indicating it captures well the strong temporal variability of regional air pollution meteorology. The global MOZART model tends to underestimate O_3 and PAN concentrations in springtime, which may lead to weakened hemispheric impacts. Although regional models improve performance in some respects, they also create new problems. Of the two regional models evaluated in this study, CMAQ tends to better capture surface photochemistry, whereas WRF-Chem better captures free tropospheric transport and chemistry. Because each has its limitations, neither can be judged "better" than MOZART for examining multi-scale processes over Asia.

We identified significant differences between regional and global models in simulating vertical mixing of trace gases to the free troposphere and subsequent outflow fluxes. Both WRF-Chem and CMAQ shows that, during multiple frontal events elevated CO, O_3 and PAN extend to the upper troposphere (6–9 km), consistent with aircraft observed distributions. The MOZART global model misplaced the pollution plumes below 4 km primarily due to its inability to capture rapid deep convection that developed along the leading edge of the convergence band during cold frontal passages. Differences between regional and global models are much larger than the variation between the online (WRF-Chem) vs. offline (CMAQ) regional models, suggesting that the limitations in the global model are induced by potential errors in convective parameterizations as well as coarse temporal and spatial resolution. Based on available data, we are only able to calculate model skill at capturing episodic outflow, but we find that CO zonal flux along 140° E is stronger in WRF-Chem throughout the study period. The pollution plumes in MOZART are diluted more quickly than observed and simulated in our regional models. Review of previous studies suggests that current large-scale global models are able to capture main features of synoptic export events, but the limitations in the ability of global models to resolve fine scale surface-to-free troposphere exchange and chemical processing would underestimate continental outflow on a consistent basis. Research needs to be undertaken to further improve the parameterizations of key export processes in large-scale climate-chemistry models, in particular orographic

ACPD
10, 109–152, 2010

forcing, intense plume rise, deep convection and associated cloud and chemical processing.

Our model analysis suggests that European anthropogenic emissions enhance CO and O_3 at Mount Hua in Central China by 40–50 ppbv and 3–5 ppbv, respectively, during typical springtime cold frontal events. Surface measurements at Mount Hua will likely be able to detect European CO enhancement in surface air. In contrast to pollution export from Asia, we find little difference in the regional vs. global model transport of European (EU) pollution into surface air over East Asia (EA). Instead, local topography, land cover and O_3-VOC-NO_x chemical sensitivity have major effects on the strength of surface O_3 responses to emission changes. For example, the O_3 response to a 20% decrease in EU emissions imported into our regional model domain exhibits a large spatial variability: strongest (0.4–0.6 ppbv) over mountainous terrain and weakest (0.1–0.3 ppbv) in megacities. The EA O_3 response to EU emission changes estimated by our regional models is approximately 0.1 ppbv lower than the global model ensemble mean (Fiore et al., 2009). We find that the uncertainty in the chemical mechanisms employed in the two regional models is equivalent to the uncertainty induced from the missing resolution-dependant processes in the global model.

These results suggest an important role for dynamic downscaling using regional climate-chemistry models in evaluating global pollution transport, both to advance our understanding of atmospheric processes, and to inform decision-making on air quality management. Due to the compensating effects on surface O_3 responses over downwind continents, future high-resolution hemispheric model analysis should provide further insights into how the export and import processes interact, and will help to narrow the uncertainty of intercontinental source-receptor relationships. Major issues that should be addressed in future research include maintaining the consistency between regional and global model physics, evaluating the role of physical parameterizations vs. resolution, and developing two-way nesting approaches. In light of the strengths and limitations of each modeling framework, there is a need for further analysis of regional processes affecting global transport and further development of models to improve skill

in all key processes. Additional analysis in areas with more extensive measurements of atmospheric constituents at the surface and in the free troposphere would also benefit understanding of hemispheric transport affecting surface air quality.

Acknowledgements. Meiyun Lin and Tracey Holloway were supported on this work by NASA grant NNX07AL36G. TRACE-P data were obtained from NASA Langley Research Center. We thank Claus Moberg for helpful comments in improving the previous version of this manuscript.

References

Akimoto, H.: Global air quality and pollution, Science, 302, 1716–1719, doi:10.1126/science.1092666, 2003.

Bolton, D.: The computation of equivalent potential temperature, Mon. Weather Rev., 108, 1046–1053, 1980.

Byun, D. W. and Schere, K. L.: Review of the governing equations, computational algorithms, and other components of the Models-3 Community Multiscale Air Quality (CMAQ) modeling system, Appl. Mech. Rev., 59, 51–77, 2006.

Carmichael, G. R., Tang, Y., Kurata, G., et al.: Regional-scale chemical transport modeling in support of the analysis of observations obtained during the TRACE-P experiment, J. Geophys. Res. 108(D21), 8823, doi:10.1029/2002JD003117, 2003.

Carmichael, G. R., Sakurai, T., Streets, D., et al.: MICS-Asia II: the model intercomparison study for Asia phase II: methodology and overview of findings, Atmos. Environ., 42(15), 3468–3490, doi:10.1016/j.atmosenv.2007.04.007, 2007.

Casper-Anenberg S., West, J., Fiore, A., et al.: Intercontinental impacts of ozone pollution on human mortality, Environ. Sci. Technol., 43(17), 6482–6487, doi:10.1021/es900518z, 2009.

Cooper, O. R., Moody, J. L., Parrish, D. D., Trainer, M., Ryerson, T. B., Holloway, J. S., Hübler, G., Fehsenfeld, F. C., and Evans M. J.: Trace gas composition of midlatitude cyclones over the western North Atlantic Ocean: a conceptual model, J. Geophys. Res., 107(D7), 4056, doi:10.1029/2001JD000901, 2002.

Cooper, O. R., Forster, C. Parrish, D., et al.: A case study of transpacific warm conveyor belt transport: influence of merging airstreams on trace gas import to North America, J. Geophys. Res., 109, D23S08, doi:10.1029/2003JD003624, 2004.

Cotton, W. R., Alexander, G. D., Hertenstein, R., Walko, R. L., McAnelly, R. L., and Nicholls, M.: Cloud venting – a review and some new global annual estimates, Earth-Sci. Rev., 39, 169–206, 1995.

Doherty, R. M., Stevenson, D. S., Collins, W. J., and Sanderson, M. G.: Influence of convective transport on tropospheric ozone and its precursors in a chemistry-climate model, Atmos. Chem. Phys., 5, 3205–3218, 2005, http://www.atmos-chem-phys.net/5/3205/2005/.

Ding, A., Wang, T., Xue, L., et al.: Transport of North China air pollution by midlatitude cyclones: Case study of aircraft measurements in summer 2007, J. Geophys. Res., 114, D08304, doi:10.1029/2008JD011023, 2009.

Duncan, B. N., Bey, I., Chin, M., Mickley, L. J., Fairlie, T. D., Martin, R. V., and Matsueda, H.: Indonesian wildfires of 1997: impact on tropospheric chemistry, J. Geophys. Res., 108(D15), 4458, doi:10.1029/2002JD003195, 2003.

Dunlea, E. J., DeCarlo, P. F., Aiken, A. C., Kimmel, J. R., Peltier, R. E., Weber, R. J., Tomlinson, J., Collins, D. R., Shinozuka, Y., McNaughton, C. S., Howell, S. G., Clarke, A. D., Emmons, L. K., Apel, E. C., Pfister, G. G., van Donkelaar, A., Martin, R. V., Millet, D. B., Heald, C. L., and Jimenez, J. L.: Evolution of Asian aerosols during transpacific transport in INTEX-B, Atmos. Chem. Phys., 9, 7257–7287, 2009, http://www.atmos-chem-phys.net/9/7257/2009/.

Ellingsen, K., Gauss, M., Van Dingenen, R., Dentener, F. J., Emberson, L., Fiore, A. M., Schultz, M. G., Stevenson, D. S., Ashmore, M. R., Atherton, C. S., Bergmann, D. J., Bey, I., Butler, T., Drevet, J., Eskes, H., Hauglustaine, D. A., Isaksen, I. S. A., Horowitz, L. W., Krol, M., Lamarque, J. F., Lawrence, M. G., van Noije, T., Pyle, J., Rast, S., Rodriguez, J., Savage, N., Strahan, S., Sudo, K., Szopa, S., and Wild, O.: Global ozone and air quality: a multi-model assessment of risks to human health and crops, Atmos. Chem. Phys. Discuss., 8, 2163–2223, 2008, http://www.atmos-chem-phys-discuss.net/8/2163/2008/.

Emmerson, K. M. and Evans, M. J.: Comparison of tropospheric gas-phase chemistry schemes for use within global models, Atmos. Chem. Phys., 9, 1831–1845, 2009, http://www.atmos-chem-phys.net/9/1831/2009/.

Fang, Y., Fiore, A. M., Horowitz, L. W., Gnanadesikan, A., Levy, H., Hu, Y., and Russell, A. G.: Estimating the contribution of strong daily export events to total pollutant export from the United States in summer, J. Geophys. Res., 114, D23302, doi:10.1029/2008JD010946,

2009.
Fast J. D., Gustafson Jr., W. I., Easter, R. C., Zaveri, R. A., Barnard, J. C., Chapman, E. G., and Grell, G. A.: Evolution of ozone, particulates, and aerosol direct forcing in an urban area using a new fully-coupled meteorology, chemistry, and aerosol model, J. Geophys. Res., 111, D21305, doi:10.1029/2005JD006721, 2006.
Fehsenfeld, F. C., Ancellet, G., Bates, T. S., et al.: International Consortium for Atmospheric Research on Transport and Transformation (ICARTT): North America to Europe – Overview of the 2004 summer field study, J. Geophys. Res., 111, D23S01, doi:10.1029/2006JD007829, 2006.
Fiedler, V., Nau, R., Ludmann, S., Arnold, F., Schlager, H., and Stohl, A.: East Asian SO_2 pollution plume over Europe - Part 1: Airborne trace gas measurements and source identification by particle dispersion model simulations, Atmos. Chem. Phys., 9, 4717–4728, 2009, http://www.atmos-chem-phys.net/9/4717/2009/.
Fiore, A. M., Jacob, D. J., Bey, I., Yantosca, R. M., Field, B. D., Fusco, A. C., and Wilkinson, J. G.: Background ozone over the United States in summer: origin, trend, and contribution to pollution episodes, J. Geophys. Res., 107(D15), 4275, doi:10.1029/2001JD000982, 2002.
Fiore, A. M., Dentener, F., Wild, O., et al.: Mutimodel estimates of intercontinental source-receptor relationships for ozone pollution, J. Geophys. Res., 114, D04301, doi:10.1029/2008JD010816, 2009.
Garreaud, R. D.: Subtropical cold surges: regional aspects and global distribution, Int. J. Climatol., 21, 1181–1197, 2001.
Grell, G. A., Peckham, S. E., Schmitz, R., McKeen, S. A., Frost, G., Skamarock W. C., and Eder, B.: Fully coupled online chemistry within the WRF model, Atmos. Environ., 39, 6957–6975, 2005.
Grell, G. A. and Dévényi, D.: A generalized approach to parameterizing convection combining ensemble and data assimilation techniques, Geophys. Res. Lett., 29(14), 1693, doi:10.1029/2002GL015311, 2002.
He, Y. J., Uno, I., Wang, Z. F., Pochanart, P., Li, J., and Akimoto, H.: Significant impact of the East Asia monsoon on ozone seasonal behavior in the boundary layer of Eastern China and the west Pacific region, Atmos. Chem. Phys., 8, 7543–7555, 2008, http://www.atmos-chem-phys.net/8/7543/2008/.
Heald, C. L., Jacob, D. J., Fiore, A. M., et al: Asian outflow and transpacific transport of carbon monoxide and ozone pollution: An integrated satellite, aircraft, and model perspective, J.

Geophys. Res., 108, D24, 4804–4820, doi:10.1029/2003JD003507, 2003.
Henne, S., Furger, M., Nyeki, S., Steinbacher, M., Neininger, B., de Wekker, S. F. J., Dommen, J., Spichtinger, N., Stohl, A., and Prévôt, A. S. H.: Quantification of topographic venting of boundary layer air to the free troposphere, Atmos. Chem. Phys., 4, 497–509, 2004, http://www.atmos-chem-phys.net/4/497/2004/.
Henne, S., Dommen, J., Neininger, B., et al.: Influence of mountain venting in the Alps on the ozone chemistry of the lower free troposphere and the European pollution export, J. Geophys. Res., 110, D22307, doi:10.1029/2005JD005936, 2005.
Hess, P. G.: A comparison of two paradigms: the relative global roles of moist convective versus nonconvective transport, J. Geophys. Res., 110, D20302, doi:10.1029/2004JD005456, 2005.
Holloway, T., Sakurai T., Han, Z., et al.: MICS-Asia II: impacts of global emissions on regional air quality in Asia, Atmos. Environ., 42(15), 3543–3561, doi:10.1016/j.atmosenv.2007.10.022, 2007.
Holtslag, A. A. M. and Boville, B. A.: Local versus nonlocal boundary layer diffusion in a global climate model, J. Climate, 6, 1825–1842, 1993.
Hong, S. Y., Noh, Y., and Dudhia, J.: A new vertical diffusion package with an explicit treatment of entrainment processes, Mon. Weather Rev., 134, 2318–2341, 2006.
Horowitz, L. W., Walters, S., Mauzerall, D. L., et al.: A global simulation of tropospheric ozone and related tracers: description and evaluation of MOZART, version 2, J. Geophys. Res., 108(D24), 4784, doi:10.1029/2002JD002853, 2003.
Hudman, R. C., Jacob, D. J., Turquety, S., et al.: Surface and lightning sources of nitrogen oxides over the United States: magnitudes, chemical evolution, and outflow, J. Geophys. Res., 112, D12S05, doi:10.1029/2006JD007912, 2007.
Jacob, D. J., Crawford, J. H., Kelb, M. M., Connors, V. S., Bendura, R. J., Raper, J. L., Sachse, G. W., Gille, J. C., Emmons, L., and Heald, C. L.: Transport and chemical evolution over the Pacific (TRACE-P) aircraft mission: design, execution and first results, J. Geophys. Res., 108(D20), 9000, doi:10.1029/2002JD003276, 2003.
Jaffe, D. A., Anderson, T., Covert, D., Kotchenruther, R., Trost, B., Danielson, J., Simpson, W., Berntsen, T., Karlsdottir, S., Blake, D., Harris, J., Carmichael, G., and Uno, I.: Transport of Asian air pollution to North America, Geophys. Res. Lett., 26(6), 711–714, 1999.
Jaffe, D. A., Snow, J., and Cooper, O.: The 2001 Asian dust events: transport and impact on surface aerosol concentrations in the US, EOS Transactions American Geophysical Union,

84(46), 501–516, 2003.
Kiley, C. M., Fuelberg, H. E., Palmer, P. I., et al.: An intercomparison and evaluation of aircraft-derived and simulated CO from seven chemical transport models during the TRACE-P experiment, J. Geophys. Res., 108(D21), 8819–8853, 2003.
Kiley, C. M. and Fuelberg, H. E.: An examination of summertime cyclone transport processes during Intercontinental Chemical Transport Experiment (INTEX-A), J. Geophys. Res., 111, D24S06, doi:10.1029/2006JD007115, 2006.
Lawrence, M. G., von Kuhlmann, R., Salzmann, M., et al.: The balance of effects of deep convective mixing on tropospheric ozone, Geophys. Res. Lett., 30(18), 1940–1943, doi:10.1029/2003GL017644, 2003.
Lelieveld, J. and Crutzen, P.-J.: Role of deep cloud convection in the ozone budget of the troposphere, Science, 264, 1759–1761, 1994.
Lelieveld, J., Berresheim, H., Borrmann, S., et al.: Global air pollution crossroads over the Mediterranean, Science, 298(5594), 794–799, doi:10.1126/science.1075457, 2002.
Li, J., Wang, Z., Akimoto, H., Gao, C., Pochanart, P., and Wang, X.: Modeling study of ozone seasonal cycle in lower troposphere over East Asia, J. Geophys. Res., 112, D22S25, doi:10.1029/2006JD008209, 2007.
Li, Q., Jacob, D. J., Munger, J. W., Yantosca, R. M., and Parrish, D. D.: Export of NO_y from the North American boundary layer: reconciling aircraft observations and global model budgets, J. Geophys. Res., 109, D02313, doi:10.1029/2003JD004086, 2004.
Lin, M., Holloway, T., Oki, T., Streets, D. G., and Richter, A.: Multi-scale model analysis of boundary layer ozone over East Asia, Atmos. Chem. Phys., 9, 3277–3301, 2009, http://www.atmos-chem-phys.net/9/3277/2009/.
Lin, M., Oki, T., Holloway, T., Streets, D. G., Bengtsson, M., and Kanae, S.: Long-range transport of acidifying substances in East Asia – Part I: Model evaluation and sensitivity studies, Atmos. Environ., 42(24), 5939–5955, doi:10.1016/j.atmosenv.2008.04.008, 2008a.
Lin, M., Oki, T., Bengtsson, M., Kanae, S., Holloway, T., and Streets, D. G.: Long-range transport of acidifying substances in Asia – Part II: Source-receptor relationships, Atmos. Environ., 42(24), 5956–5967, doi:10.1016/j.atmosenv.2008.03.039, 2008b.
Liu, H. Y., Jacob, D. J., Bey, I., et al.: Transport pathways for Asian pollution outflow over the Pacific: interannual and seasonal variations, J. Geophys. Res., 108(D20), 8786, doi:10.1029/2002JD003102, 2003.
Moxim II, W. J., Levy, H., and Kasibhatla, P. S.: Simulated global tropospheric PAN: its transport

and impact on NO_x, J. Geophys. Res., 101(D7), 12621–12638, 1996.
NOAA: 2010 CalNex Science and Implementation Plan – Research at the Nexus of Air Quality and Climate Change, October 2008, http://www.esrl.noaa.gov/csd/calnex/, (last access: December 2009), 2008.
Parrish, D. D., Ryerson, T. B., Holloway, J. S., et al.: Fraction and composition of NO_y transported in air masses lofted from the North American continental boundary layer, J. Geophys. Res., 109, D09302, doi:10.1029/2003JD004226, 2004.
Pfister, G. G., Emmons, L. K., Hess, P., et al.: Ozone production from the 2004 North American boreal fires, J. Geophys. Res., 111, D24S07, doi:10.1029/2006JD007695, 2006.
Pochanart, P., Akimoto, H., Kajii, Y., et al: Regional background ozone and carbon monoxide variations in remote Siberia/East Asia, J. Geophys. Res., 108(D1), 4028–4045, doi:10.1029/2001JD001412, 2003.
Real, E., Law, K. S., Weinzierl, B., et al. : Process influencing ozone levels in Alaskan forest fire plumes during long-range transport over the North Atlantic, J. Geophys. Res., 112, D10S41, doi:10.1029/2006JD007576, 2007.
Reidmiller, D. R., Fiore, A. M., Jaffe, D. A., Bergmann, D., Cuvelier, C., Dentener, F. J., Duncan, B. N., Folberth, G., Gauss, M., Gong, S., Hess, P., Jonson, J. E., Keating, T., Lupu, A., Marmer, E., Park, R., Schultz, M. G., Shindell, D. T., Szopa, S., Vivanco, M. G., Wild, O., and Zuber, A.: The influence of foreign vs. North American emissions on surface ozone in the US, Atmos. Chem. Phys., 9, 5027–5042, 2009, http://www.atmos-chem-phys.net/9/5027/2009/.
Richter, A., Burrows, J. P., Nuss, H., Granier, C., and Niemeier, U.: Increase in tropospheric nitrogen dioxide over China observed from space, Nature, 437(7055), 129–132, 2005.
Sanderson, M., Dentener, F. J., Fiore, A. M., et al.: A multi-model study of the hemispheric transport and deposition of oxidised nitrogen, Geophys. Res. Lett., 35, L17815, doi:10.1029/2008GL035389, 2008.
Seinfeld, J. H. and Pandis, S. N.: Atmospheric Chemistry and Physics: From Air Pollution to Climate Change, Wiley, New York, 215–225, 2006.
Simpson, D., Guenther, A., Hewitt, C. N., and Steinbrecher, R.: Biogenic emissions in Europe. 1. Estimates and uncertainties, J. Geophys. Res., 100D, 22875–22890, 1995.
Guenther, A., Zimmerman, P., and Wildermuth, M.: Natural volatile organic compound emission rate estimates for US woodland landscapes, Atmos. Environ., 28, 1197–1210, 1994.
Singh, H. B., Brune, W. H., Crawford, J. H., Jacob, D. J., and Russell, P. B.: Overview of the

summer 2004 Intercontinental Chemical Transport Experiment – North America (INTEX-A), J. Geophys. Res., 111, D24S01, doi:10.1029/2006JD007905, 2006.
Singh, H. B., Brune, W. H., Crawford, J. H., Flocke, F., and Jacob, D. J.: Chemistry and transport of pollution over the Gulf of Mexico and the Pacific: spring 2006 INTEX-B campaign overview and first results, Atmos. Chem. Phys., 9, 2301–2318, 2009, http://www.atmos-chem-phys.net/9/2301/2009/.
Streets, D. G., Bond, T. C., Carmichael, G. R., Fernandes, S. D., Fu, Q., He, D., Klimont, Z., Nelson, S. M., Tsai, N. Y., Wang, M. Q., Woo, J. H., and Yarber, K. F.: An inventory of gaseous and primary aerosol emissions in Asia in the year 2000, J. Geophys. Res., 108(D21), 8809, doi:10.1029/2002JD003093, 2003.
Streets, D. G., Zhang, Q., Wang, L., He, K., Hao, J., Wu, Y., Tang, Y., and Carmichael, G. R.: Revisiting China's CO emissions after the Transport and Chemical Evolution over the Pacific (TRACE-P) mission: synthesis of inventories, atmospheric modeling, and observations, J. Geophys. Res., 111, D14306, doi:10.1029/2006JD007118, 2006.
Stohl, A., Eckhardt, S., Forster, C., James, P., and Spichtinger, N.: On the pathways and timescales of intercontinental air pollution transport, J. Geophys. Res., 107(D23), 4684, doi:10.1029/2001JD001396, 2002.
Tanimoto, H.: Increase in springtime tropospheric ozone at a mountainous site in Japan for the period 1998–2006, Atmos. Environ., 43, 1358–1363, 2009.
Tie, X., Madronich, S., Li, G., Ying, Z., Weinheimer, A., Apel, E., and Campos, T.: Simulation of Mexico City plumes during the MIRAGE-Mex field campaign using the WRF-Chem model, Atmos. Chem. Phys., 9, 4621–4638, 2009, http://www.atmos-chem-phys.net/9/4621/2009/.
Task Force on Hemispheric Transport of Air Pollution: Hemispheric transport of air pollution 2007 interim report, edited by: Keating, T. J. and Zuber, A., Air Pollut. Stud. 16, U.N. Econ. Comm. for Europe, New York, 2007.
Turquety, S., Logan, J. A., Jacob, D. J., Hudman, R. C., Leung, F. Y., Heald, C. L., Yantosca, R. M., Wu, S., Emmons, L. K., Edwards, D. P., and Sachse, G. W.: Inventory of boreal fire emissions for North America in 2004: importance of peat burning and pyroconvective injection, J. Geophys. Res., 112, D12S03, doi:10.1029/2006JD007281, 2007.
Uno, I., Carmichael, G. R., Streets, D. G., et al.: Regional chemical weather forecasting system CFORS: model descriptions and analysis of surface observations at Japanese island stations during the ACE-Asia experiment, J. Geophys. Res., 108(D23), 8668,

doi:10.1029/2002JD002845, 2003.
van der Werf, G. R., Randerson, J. T., Giglio, L., Collatz, G. J., Kasibhatla, P. S., and Arellano Jr., A. F.: Interannual variability in global biomass burning emissions from 1997 to 2004, Atmos. Chem. Phys., 6, 3423–3441, 2006, http://www.atmos-chem-phys.net/6/3423/2006/.
Wild, O., Pochanart, P., and Akimoto, H.: Trans-Eurasian transport of ozone and its precursors, J. Geophys. Res., 109, D11302, doi:10.1029/2003JD004501, 2004.
Yienger, J., Galanter, M., Holloway, T., Phandis, M., Guttikunda, S., Carmichael, G., Moxim, W., and Levy II, H.: The episodic nature of air pollution transport from Asia to North America, J. Geophys. Res., 105(D22), 26931–26945, 2000.
Zaveri, R. A. and Peters, L. K.: A new lumped structure photochemical mechanism for large-scale applications, J. Geophys. Res., 104(D23), 30387–30415, 1999.
Zhang, L., Jacob, D. J., Boersma, K. F., Jaffe, D. A., Olson, J. R., Bowman, K. W., Worden, J. R., Thompson, A. M., Avery, M. A., Cohen, R. C., Dibb, J. E., Flock, F. M., Fuelberg, H. E., Huey, L. G., McMillan, W. W., Singh, H. B., and Weinheimer, A. J.: Transpacific transport of ozone pollution and the effect of recent Asian emission increases on air quality in North America: an integrated analysis using satellite, aircraft, ozonesonde, and surface observations, Atmos. Chem. Phys., 8, 6117–6136, 2008, http://www.atmos-chem-phys.net/8/6117/2008/.
Zhang, M. G., Uno, I., Carmichael, G. R., et al.: Large-scale structure of trace gas and aerosol distributions over the western Pacific Ocean during the Transport and Chemical Evolution Over the Pacific (TRACE-P) experiment, J. Geophys. Res., 108(D21), doi:10.1029/2002JD002946, 2003.
Zhang, Q., Streets, D. G., He., K., et al.: NO_x emission trends for China, 1995–2004: the view from the ground and the view from space, J. Geophys. Res., 112, D22306, doi:10.1029/2007JD008684, 2007.
Zhao, C., Wang, Y., Choi, Y., and Zeng, T.: Summertime impact of convective transport and lightning NO_x production over North America: modeling dependence on meteorological simulations, Atmos. Chem. Phys., 9, 4315–4327, 2009, http://www.atmos-chem-phys.net/9/4315/2009/.

Table 1. Total emissions of ozone precursors over East Asia (15–50° N, 95–160° E) in March in the individual models[a].

MODEL	NOx (Gg N)	CO (Gg)	NMVOC (Gg C)
MOZART	404.8	12 157.5	2445.0
WRF-Chem	453.2	12 775.5	1258.2
CMAQ	464.8	13 307.5	2516.4

[a] Emissions for WRF-Chem do not include biogenic sources since they are calculated on-line. Supplementary Figs. S1 and S2 (http://www.atmos-chem-phys-discuss.net/10/109/2010/acpd-10-109-2010-supplement.pdf) compare spatial distributions of anthropogenic (including biomass burning) and biogenic emissions, respectively.

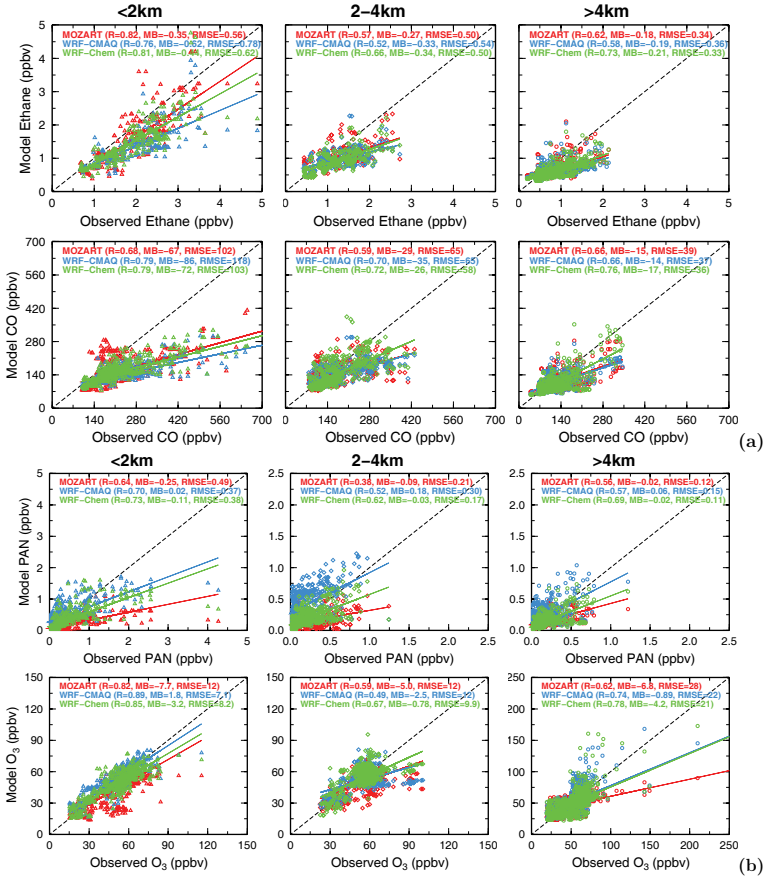

Fig. 1. **(a)**Comparision of measured (5-min merged) and modeled CO and ethane along the TRACE-P flight tracks in March 2001. Individual points correspond to flight sections at altitudes below 2 km (left panel), 2–4 km (middle panel), and above 4 km (right panel). Correlation coefficients (*R*), mean bias (MB, in ppbv) and root mean square error (RMSE, in ppbv) are calculated for each model: MOZART (red), WRF-CMAQ (blue), and WRF-Chem (green). **(b)** Same as Fig. 1a, but for photochemical oxidants O_3 and PAN.

ACPD
10, 109–152, 2010

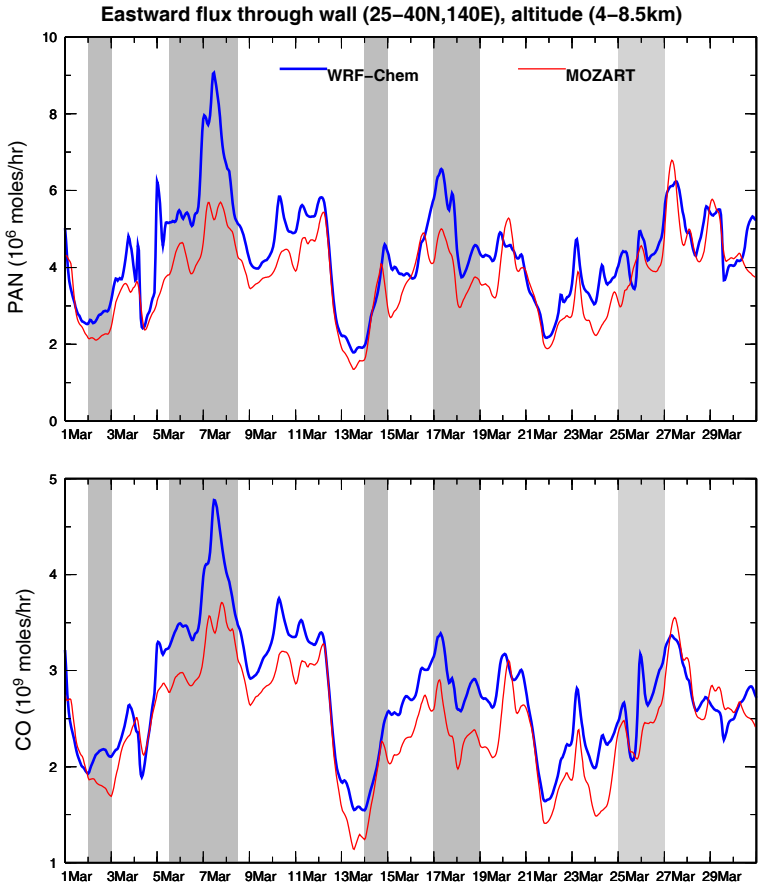

Fig. 2. Comparison of MOZART and WRF-Chem calculated zonal fluxes of CO and PAN along 140° E that is integrated over 4–8.5 km altitudes and 25°–40° N latitudes. Episodes of cold frontal passages in March 2001 are highlighted in gray.

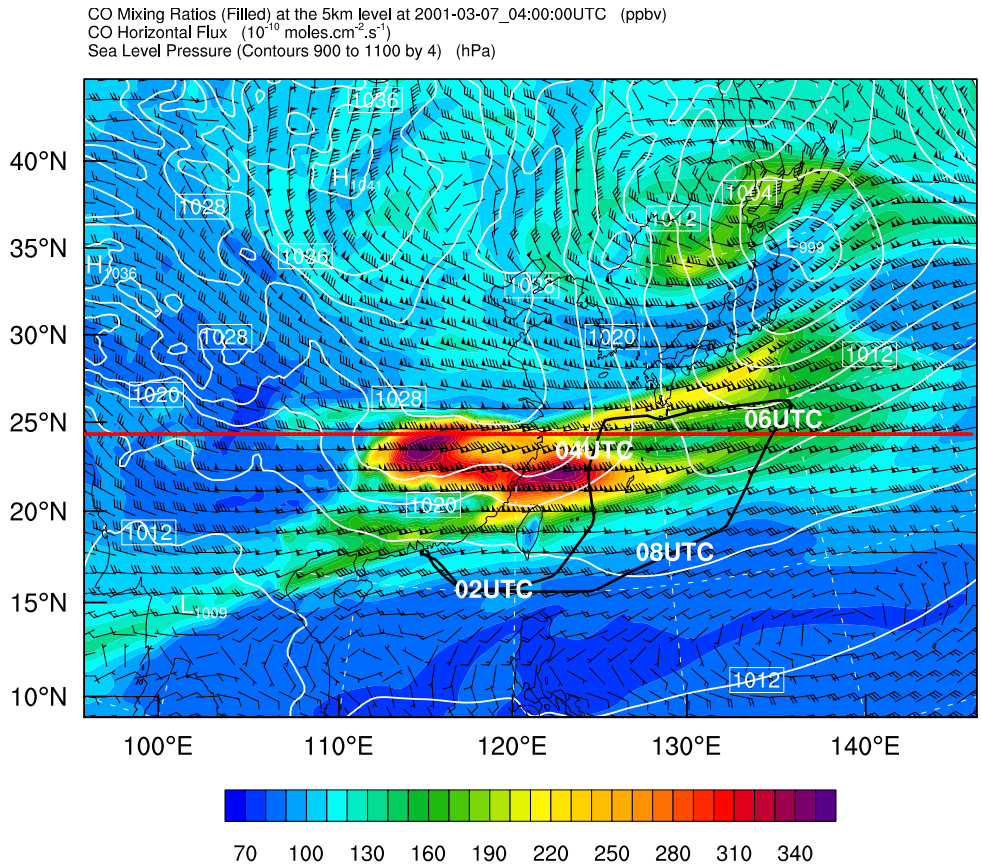

Fig. 3. WRF-Chem simulated CO mixing ratios (filled) and horizontal flux at the 5 km level superimposed with sea level pressure (contours) at 04:00 UTC on 7 March. The red horizontal line indicates the location of vertical cross-section shown in Fig. 4. The thick black line denotes the flight track and UTC of the NASA DC8.

ACPD
10, 109–152, 2010

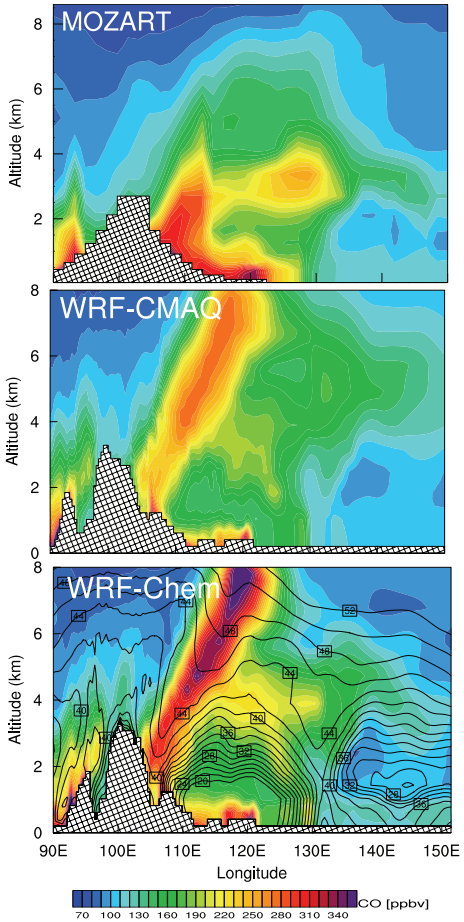

Fig. 4. Comparison of model simulated convective and updraft mixing of CO in association with the passage of the cyclonic wave during 6–7 March. Shown are vertical distributions of CO (filled) and equivalent potential temperature (contours) along ~25° N at 00:00 UTC on 7 March.

ACPD
10, 109–152, 2010

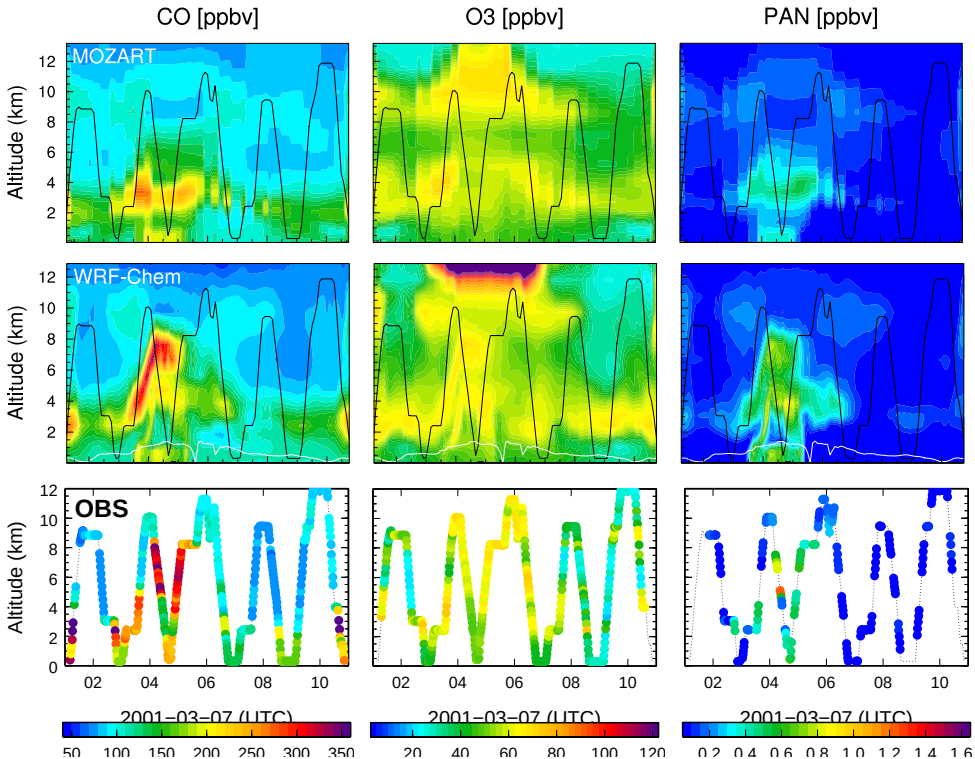

Fig. 5. Observed (1-min merged) and predicted vertical profiles of trace gases along the DC-8 flight track on 7 March during the TRACE-P campaign. The flight path is shown as black lines. White lines indicate boundary layer heights.

ACPD
10, 109–152, 2010

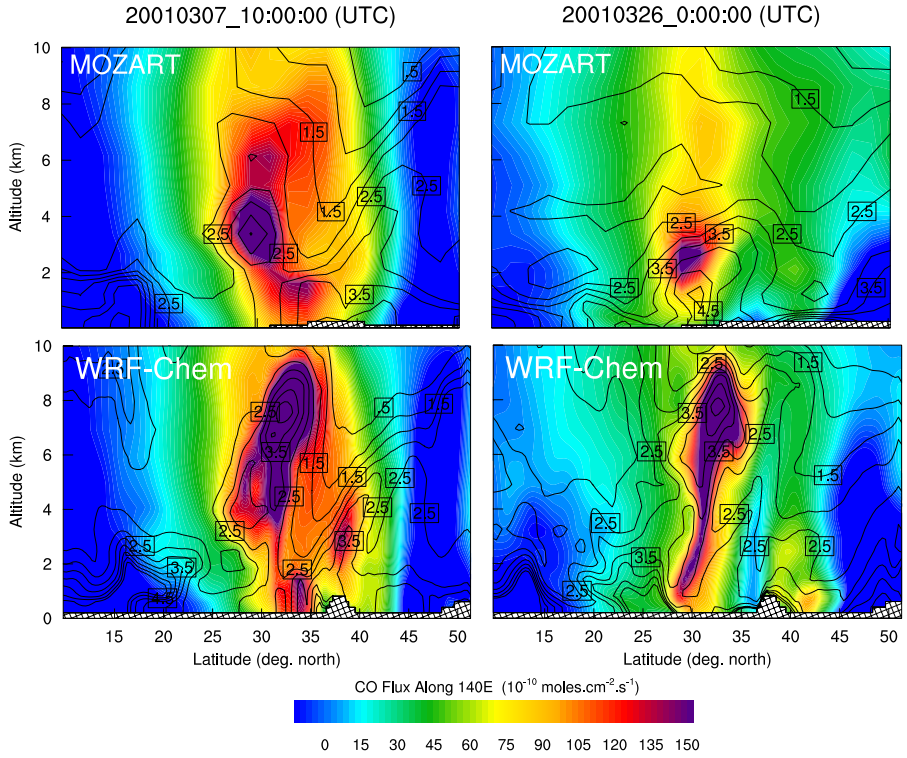

Fig. 6. Comparison of MOZARTand WRF-Chem simulated vertical profiles of CO zonal flux along 140° E for selected episodes. The CO/O_3 ratio in the outflow pollution plume is shown as contours from 0.5 to 5 by 0.5.

ACPD
10, 109–152, 2010

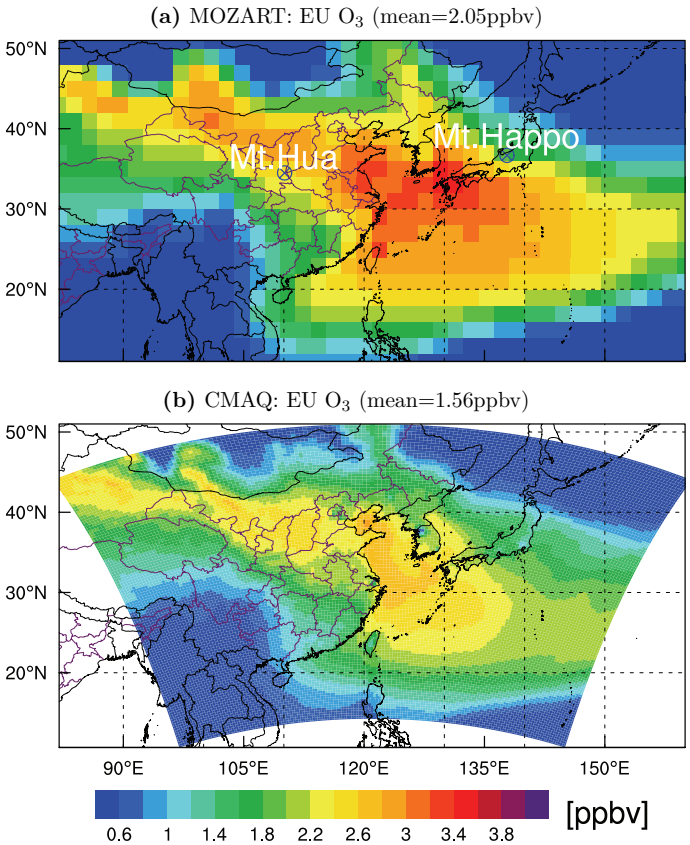

Fig. 7. European enhancement on surface ozone in East Asia averaged over 1–15 March. Note that the response to 20% emission decreases is multiplied by a factor of five, same in Figs. 8 and 9. Circles in the upper panel denote Mount Hua (34.5° N, 110.1° E, 2064 m) in Central China and Mount Happo (36.7° N, 137.8° E, 1850 m) in Central Japan.

ACPD
10, 109–152, 2010

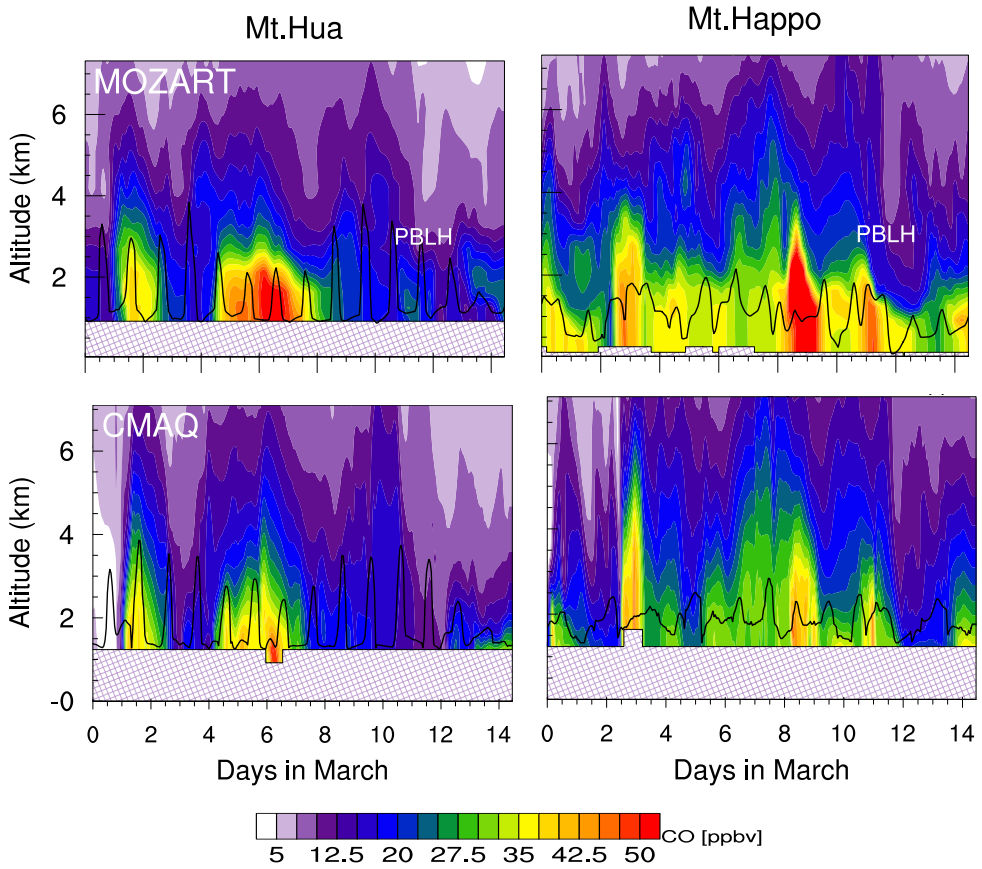

Fig. 8. Time evolution of the vertical profiles of European CO over China (Mt. Hua) and Japan (Mt. Happo) during 1–14 March. The black line denotes the boundary layer depth. The hatched areas indicate that local surface pressure is below the bottom pressure level used for vertical interpolation, thus the average height of hatched areas can roughly represent local terrain heights assumed in the model.

ACPD
10, 109–152, 2010

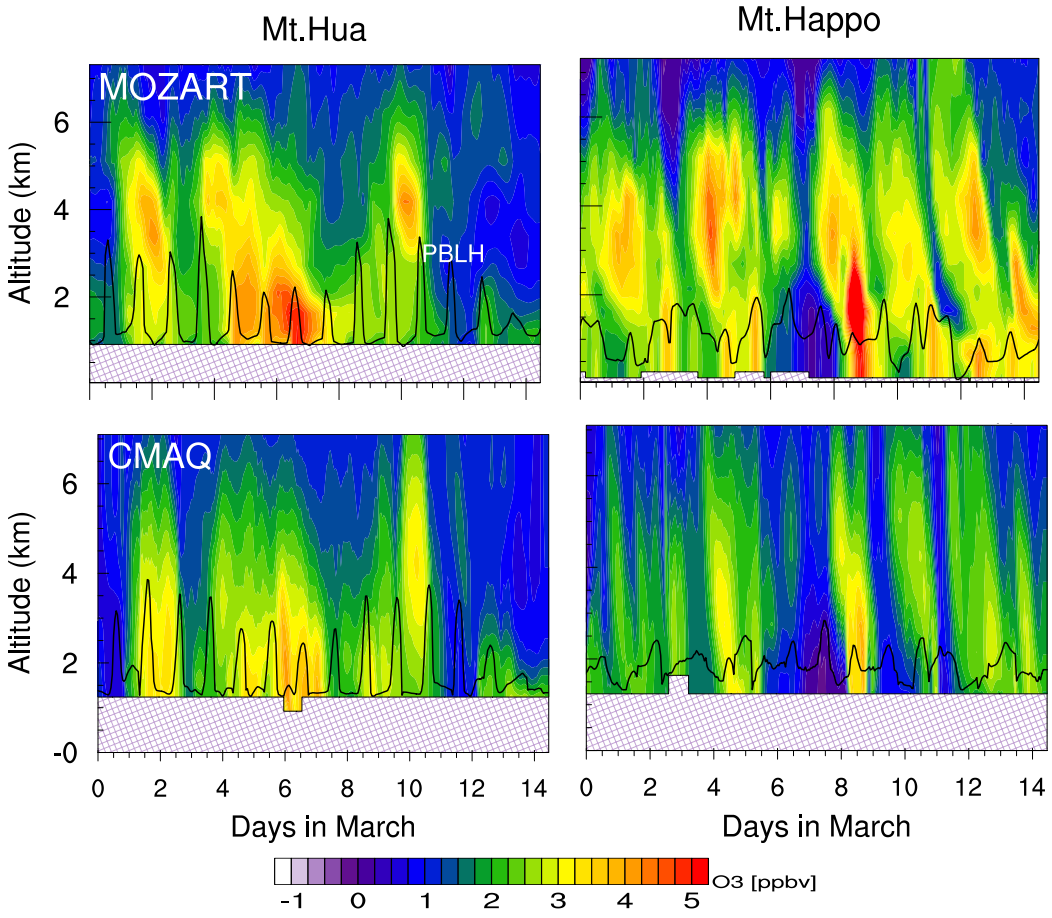

Fig. 9. Same as Fig. 8, but for ozone.

ACPD
10, 109–152, 2010